EPJ Web of Conferences **40**, 06004 (2013)
DOI: 10.1051/epjconf/20134006004

Microstructure and magnetic properties of hard magnetic $Pr_9Fe_{52}Co_{13}Zr_1Ti_3B_{22}$ alloy ribbons

K. Pawlik[1]

[1]Institute of Physics, Częstochowa University of Technology, al. Armii Krajowej19, 42-201 Częstochowa, Poland

Abstract. In the present work the phase constitution, microstructure and magnetic properties of the $Pr_9Fe_{52}Co_{13}Zr_1Ti_3B_{22}$ alloy ribbons in the as-cast state and subjected to short time annealing were investigated. The ribbons were obtained by melt-spinning technique (with the velocity of the copper roll surface of 15 m/s). Subsequently, the samples were annealed for 5 min at temperatures ranging from 923 to 1013K. The ribbon samples in as-cast state were fully amorphous and exhibited soft magnetic properties. Annealing at 923K resulted in partial devitrification of samples that has not changed considerably their magnetic properties. Heat treatment of specimens at higher temperatures caused the increase of volume fractions of hard magnetic phase, which was accompanied by significant changes of their hysteresis loops. The evolution of microstructure was studied by transmission electron microscopy TEM. Magnetic interactions between the grains of crystalline phases of selected samples were investigated basing on the deltaM plots determined from recoil curves.

1 Introduction

Since the discovery of highly anisotropic $Nd_2Fe_{14}B$ phase responsible for excellent magnetic properties of Nd-Fe-B magnets, a numerous techniques for processing nanocrystalline magnets were developed. The most frequently used techniques for mass production are: sintering [1], mechanical alloying [2] and HDDR [3]. However, especially attractive are some variants of rapid solidification technologies. These processes allow to obtain directly quenched nanocrystalline bulk magnets or to derive them from bulk glassy precursors [4, 5]. As the result significant reduction of costs due to shortening of processing time and saving the energy required for producing nanocrystalline microstructure can be achieved. The important advantage of the Fe-based glassy alloys are the possibilities of tailoring their magnetic properties by appropriate chemical admixture and annealing [6]. A very good hard magnetic properties were revealed for the melt-spun ribbon samples of RE-Fe-B alloys (RE – rare earth elements) [7] subjected to heat treatment. Studies carried out on $Pr_9Fe_{58-x}Co_{13}Zr_1Nb_4B_{15+x}$ (x=0, 3, 6, 8) alloys [8] shown improvement of their glass forming abilities with the increase of boron content. For this type of alloys the magnetic interactions between grains in nanocrystalline magnets derived from bulk glassy precursors were investigated in [9]. Furthermore, significant impact of Zr, Nb or W admixtures on glass forming abilities of RE-Fe-B alloys were demonstrated in [10, 11]. Hard magnetic properties are strongly related both to the phase constitution and microstructure of the alloy. Presence of large volume fraction of hard magnetic phase is of great importance, however the uniform nanocrystalline microstructure is another key factor. Both of them can by tailored by the chemical composition of the alloy. It was shown in [11] that in order to hinder the grain growth during annealing, the admixture of Ti and C to the alloy composition give a good outcome. Such modification led to enhancement of polarization remanence J_r, coercive field ${}_JH_c$ and maximum energy product $(BH)_{max}$. In the present studies the $Pr_9Fe_{52}Co_{13}Zr_1Ti_3B_{22}$ alloy ribbons, with large boron content and admixture of Zr and Ti were investigated. We have demonstrated previously [5, 8, 15] that such addition promote good glass forming abilities and retards grain growth during annealing. The aim of present work was to investigate the influence of annealing conditions on magnetic properties, phase constitution and microstructure of rapidly solidified ribbons. Furthermore, the magnetic interactions between grains were studied.

2 Sample preparation and experimental methods

The $Pr_9Fe_{52}Co_{13}Zr_1Ti_3B_{22}$ base alloy was prepared by arc-melting of constituent elements of high purity with addition of pre-alloy Fe-B of known composition. The ingot samples were re-melted several times under an

argon atmosphere in order to get uniform elements distribution. Subsequently, the ribbon samples were produced by single roll melt-spinning technique under the argon atmosphere at linear velocity of the copper roll surface of ~15m/s. This allowed to obtain ribbons of average thicknesses of ~70μm. The rapidly solidified samples were sealed off in the quartz tubes under the Ar atmosphere and subjected to the short time annealing at the temperature ranging from 923 K to 1033 K for 5 min.

The phase constitution of the annealed samples was studied by X-ray diffractometry (XRD) with CuKα radiation. The microstructure was revealed by transmission electron microscopy (TEM). Magnetic properties were examined at room temperature using vibrating sample magnetometer at external magnetic field up to 2T.

3 Results and discussion

In figure 1 the XRD scans are presented for ribbon in as-cast state and subjected to annealing at various temperatures from 923K to 953K for 5 min. For as-cast sample a wide bump in the range of 2Θ between 35 and 50 deg was observed. Annealing at 923K for 5 min resulted in slight modification of the phase constitution.

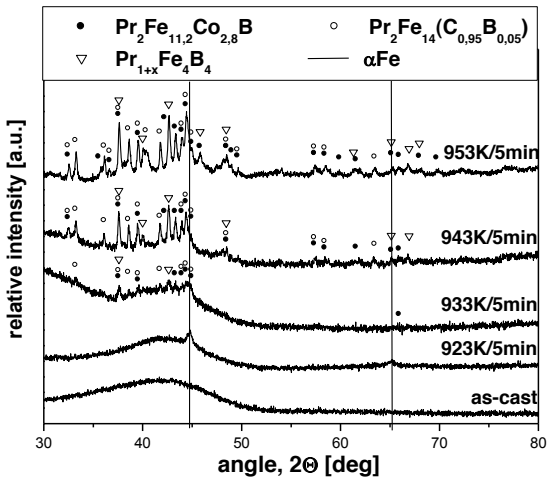

Fig.1. The X-ray diffraction patterns for $Pr_9Fe_{52}Co_{13}Zr_1Ti_3B_{22}$ alloy ribbons in the as-cast state and subjected to annealing at various temperatures.

The broad peaks of low intensities identified as α-Fe phase become apparent in the XRD scan. Significant change of the phase constitution was evidenced for the ribbons annealed at 933K for 5 min. At this annealing temperature the growth of α-Fe was retarded in favour of other crystalline phases. A number of low intensity peaks corresponding to those phases together with wide bump from the amorphous matrix were shown in the XRD scan for ribbon annealed at 933K. Annealing at higher temperatures resulted in the increase of peaks intensities, however no change of their angular positions was observed. This suggests that heat treatment at temperatures higher than 933K results in formation of the same crystalline phases. The phase analysis of ribbons annealed at this temperature range indicates presence of paramagnetic $Pr_{1+x}Fe_4B_4$ and hard magnetic $Pr_2(Fe, Co)_{14}B$ phases. An important result of this studies was the identification of peaks corresponding to not expected hard magnetic $Pr_2Fe_{14}(C_{0.95}B_{0.05})$ phase. Carbon present in the alloy composition was not intentionally added to the alloy, but came from the rubber seals in the arc-melting furnace used for synthesis of the ingot samples. Such seal decomposes and carbon evaporates at high temperatures.

In order to observe the microstructure evolution with annealing temperature the TEM images of samples annealed at 933K, 943K, 953K and 983K were collected.

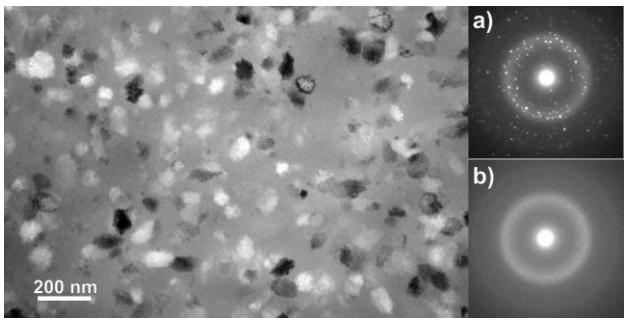

Fig.2. The microstructure of ribbon annealed at 933K together with the electron diffraction patterns from the entire visible area (a) and from the amorphous matrix (b).

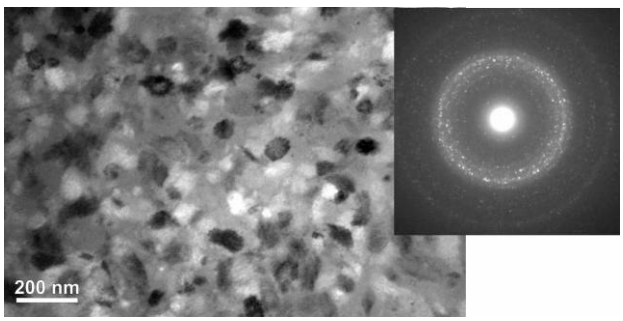

Fig.3. The microstructure of ribbon annealed at 943K together with the electron diffraction pattern from the entire visible area.

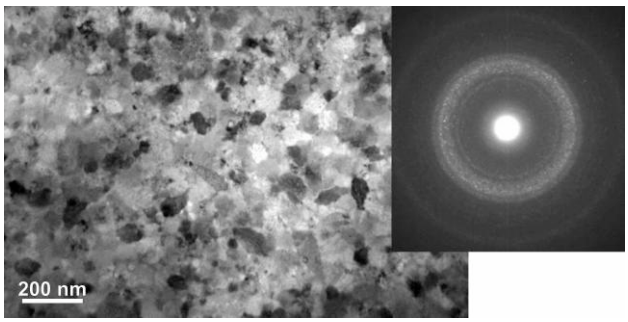

Fig.4. The microstructure of ribbon annealed at 983K together with the electron diffraction pattern from the entire visible area.

In figure 2 the selected TEM image for ribbon annealed at 933K together with the electron diffraction patterns from the entire visible area (a) and from the amorphous matrix (b) are presented. For this sample the microstructure consists of oval grains dispersed within the amorphous matrix. The mean grain diameters

measured for this sample range from 50 to 100 nm. Similar grain sizes were measured for specimens annealed at higher temperatures. In figure 3 the microstructure of the sample annealed at 943K together with the electron diffraction pattern from entire visible area were presented. The TEM studies shown that the grain sizes measured in all annealed samples were in the same range from 50 to 100 nm while the contents of crystalline phases depended on the annealing temperature. The analysis of the TEM images allowed to estimate the ratio of the regions taken by the crystalline grains to the whole picture area. For the samples annealed at 933K and 943K these ratios were about 0.39 and 0.56, respectively. The microstructure of the sample annealed at 983K together with the diffraction pattern from the entire visible area were shown in figure 4. The diffused ring originated from amorphous phase was evident, however it is expected that much smaller volume fraction is taken by this phase. Such change of microstructure has significant effect on the magnetic properties of the samples.

The influence of heat treatment of ribbons on their magnetic properties was shown in figure 5. The samples annealed at temperatures lower than 933K revealed soft magnetic properties due to low fraction of crystalline phases. An increase of annealing temperature resulted in drop of saturation magnetization J_s.

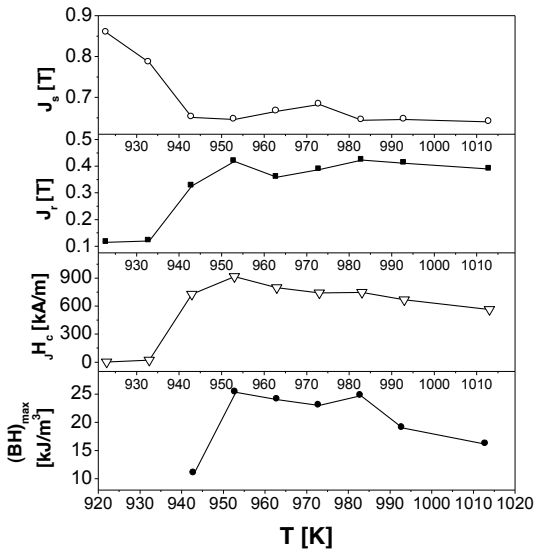

Fig.5. Saturation polarization Js, remanence Jr, coercivity $_JH_c$ and maximum energy product $(BH)_{max}$ vs. the annealing temperature T measured for ribbons of the $Pr_9Fe_{52}Co_{13}Zr_1Ti_3B_{22}$ alloy.

Additionally, the increase of coercivity and polarization remanence was observed for samples annealed at 943K. The heat treatment at higher temperatures led to continuous reduction of coercivity and almost constant remanence values. Such changes are due to the increase of the volume fraction of hard magnetic phase in expense of amorphous matrix during annealing of the ribbons.

In figure 6 the hysteresis loops for selected samples are shown. A low volume fraction of hard magnetic isolated grains in sample annealed at 933K gave a wasp-waisted hysteresis loop and low coercivity. Presence of large volume fraction of soft magnetic amorphous phase has an effect in higher value of the saturation polarization of ribbon. An increase of the annealing temperature led to significant remanence enhancement, suggesting presence of interactions between grains. Furthermore, the squerness of the hysteresis loops was improved with the increase of annealing temperature. Large volume fraction of the paramagnetic $Pr_{1+x}Fe_4B_4$ phase and change of the chemical composition of the amorphous matrix resulted in reduction of J_s and relatively low values of $(BH)_{max}$.

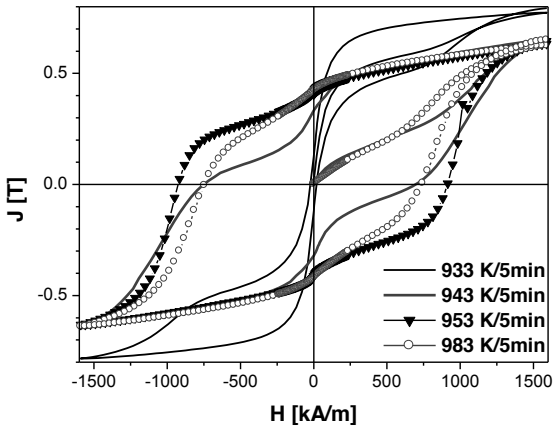

Fig.6. The hysteresis loops for $Pr_9Fe_{52}Co_{13}Zr_1Ti_3B_{22}$ alloy ribbons annealed at various temperatures.

In order to characterize the interactions between grains of crystalline phases the δM plots [12] were constructed from the recoil curves measured for selected samples in the demagnetized state and after magnetic saturation (figure 7). The magnitude of interactions between grains is described by the deviation from linear relation between the irreversible magnetization of initially saturated sample $M_{irr}^{D}(H)$ and the irreversible part of magnetization for the demagnetized one $M_{irr}^{R}(H)$, that was predicted by Stoner-Wohlfarth model [13].

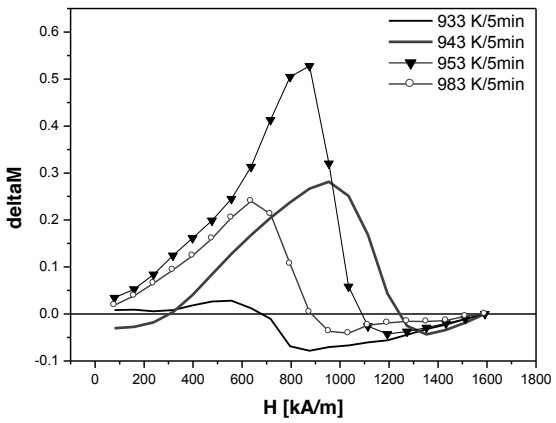

Fig.7. The δM plots for $Pr_9Fe_{52}Co_{13}Zr_1Ti_3B_{22}$ alloy ribbons annealed at various temperatures.

The value of this deviation δM for various applied magnetic fields H can be deduced from equation:

$$\delta M(H) = \{M_{irr}^{D}(H) - [M_r - 2M_{irr}^{R}(H)]\} / M_r \quad (1)$$

Here the M_r is the remanence determined from the hysteresis loop.

The strongest interactions, related to positive δM values that corresponds to exchange interactions stabilizing magnetization [14], were present in ribbons annealed at 953K. This sample exhibited the best hard magnetic properties (figures 5 and 6). For the ribbon annealed at 933K the dipolar interactions were dominant. However, low positive δM at fields lower than 700 kA/m come from exchange interactions between hard magnetic grains for which the intergrain distance is in the range of the exchange length. The negative values of δM at low magnetic fields observed for sample annealed at 943K prove the existence of dipolar interactions between grains that lessen the magnetization. Such interactions are also responsible for substantial drop of magnetic polarization on the demagnetization curve at low magnetic fields for this sample (figure 6).

4 Conclusions

The evolution of phase constitution and microstructure accompanied by the changes of magnetic properties for rapidly solidified ribbons of $Pr_9Fe_{52}Co_{13}Zr_1Ti_3B_{22}$ alloy subjected to short time annealing at various temperatures were studied. Heat treatment at 923K resulted in precipitation of α-Fe phase and soft magnetic properties of the sample. Even a small increase of annealing temperature retarded growth of α-Fe in favour of hard magnetic $Pr_2(Fe, Co)_{14}B$ and paramagnetic $Pr_{1+x}Fe_4B_4$ phases. However, the distances between most of the grains of hard magnetic phase were too long in order to provide conditions for coupling. Thus the long range dipolar interactions play dominant role for the sample annealed at 933K. The volume fractions of the crystalline components significantly increase with the annealing temperature. This has important effect in the exchange interactions between grains thus leading to improvement of magnetic properties for ribbon annealed at 943K for 5 min. This has its reflection in δM plots constructed for studied samples.

Acknowledgements

Work supported by the research project N N507 240840 financed by Polish National Science Centre in years 2011–2014

References

1. M. Sagawa, S. Fujimura, N. Togawa, H. Yamamoto, J. Matsuura, J. Appl. Phys. 55, 2083 (1984)
2. W. Kaszuwara, M. Leonowicz, M. Psoda, C. Harland, H.A. Davies, Proc. On 16th Inter. Workshop on RE Magnets and Their Applications, Sendai, p. 669, (2000)
3. P. McGuiness, C. Short, A.F. Wilson, J.R. Harris, J. Alloy. Comp. 184, 243 (1992)
4. K. Pawlik, P. Pawlik, J.J. Wysłocki, W. Kaszuwara, Acta Phys. Pol. A 113, 39, (2008)
5. P. Pawlik, K. Pawlik, J.J. Wysłocki, W. Kaszuwara, J. Ferenc, J. Alloy. Compd., DOI: 10.1016/j.jallcom.2011.12.005
6. P. Pawlik, K. Pawlik, H.A. Davies, W. Kaszuwara, J.J. Wysłocki, J. Magn. Magn. Mater. 316, e124 (2007)
7. A. Manaf, R. A. Buckley, H. A. Davies, M. Leonowicz, J. Magn. Magn. Mat. 101, 360 (1991)
8. K. Pawlik, P. Pawlik, J.J. Wysłocki, Acta Phys. Pol. A, 118, 900 (2010)
9. K. Pawlik, P. Pawlik, J.J. Wysłocki, W. Kaszuwara, J. Alloy. Compd., DOI: 10.1016/j.jallcom.2011.12.003
10. B. Xiaoqian, Z. Jie, L. Wei, G. Xuexu, Z. Shouzeng, J. Rare Earth, 27, 843, (2009)
11. S. Hirosawa, H. Kanekiyo, Y. Shigemoto, T. Miyoshi, Proc. 18th Inter. Work. High Performance Magnets and their Applications, Annecy pp. 655 (2004)
12. P.E. Kelly, K. O'Grady, P.I. Mayo, R.W. Chantrell, IEEE Trans. Magn., 25, 3881 (1989)
13. E. P. Wohlfarth, J. Appl. Phys., 29, 595 (1958)
14. P.I. Mayo, R.M. Erkkila, A. Bradbury, R.W. Chantrell, IEEE Trans. Magn., 26, 1894 (1990)
15. P. Pawlik, K. Pawlik, H.A. Davies, W. Kaszuwara, J.J. Wysłocki, J. Magn. Magn. Mater., 316, e124 (2007)